INL/JOU-25-85649-Revision-0

Quantitative Encapsulation and Homogeneity Assessment of SolGel Based Nuclear Explosive Debris Simulants

November 2025

Justin Teryl Cooper, Mathew S Snow, Tommy Holschuh, Jacob L Brookhart, Tashi Parsons-Davis, Jennifer Shusterman, Todd Wooddy, Jessica Meiers

Changing the World's Energy Future

INL is a U.S. Department of Energy National Laboratory operated by Battelle Energy Alliance, LLC

INL/JOU-25-85649-Revision-0

Quantitative Encapsulation and Homogeneity Assessment of SolGel Based Nuclear Explosive Debris Simulants

Justin Teryl Cooper, Mathew S Snow, Tommy Holschuh, Jacob L Brookhart, Tashi Parsons-Davis, Jennifer Shusterman, Todd Wooddy, Jessica Meiers

November 2025

Idaho National Laboratory
Idaho Falls, Idaho 83415

http://www.inl.gov

Prepared for the
U.S. Department of Energy
Under DOE Idaho Operations Office
Contract DE-AC07-05ID14517

Quantitative Encapsulation and Homogeneity Assessment of Sol-gel Based Nuclear Explosive Debris Simulants

Justin Cooper[1*], Tashi Parsons-Davis[2], Jennifer Shusterman[2], Todd Wooddy[2], Jacob Brookhart[1], Jessica Meiers[1], Thomas Holschuh[2], Mathew Snow[1]

[1]*Idaho National Laboratory, 1765 N. Yellowstone Hwy, Idaho Falls, Idaho 83415, United States of America*

[2]*Lawrence Livermore National Laboratory, 7000 East Ave, Livermore, CA, 94550, United States of America*

**Corresponding Author: justin.cooper@inl.gov*

Abstract

Nuclear explosive debris simulants are an important material in training and validating aspects of post-detonation nuclear forensic processes. Realistic simulants should replicate several aspects of nuclear explosive debris such as the size, shape, color, density, and chemical and radiological properties. Silica particles produced via sol-gel synthesis have recently been found to successfully reproduce many of these parameters including the controllable incorporation of radionuclide content. However, to be useful as a benchmarking material for validation and verification of laboratory methodologies, radionuclide content from batch-to-batch must be reproducible. In this work, we explore the variance in radionuclide distribution incorporated into sol-gel benchmarking materials with respect to sample subdivision. Results will help inform the sample sizes required to minimize variance between samples.

Keywords

Nuclear Forensics, Nuclear Explosive Debris Simulants, Reference Materials, Sol-gel, Homogeneity, Encapsulation.

Introduction

Post-detonation nuclear forensic analysis is the scientific evaluation of nuclear debris produced from a nuclear explosion, with the intent to assist the attribution of the event. The maintenance of a robust and reliable nuclear forensic capability is a key component to countering nuclear terrorism and forms an integral objective of international engagement.[1-5]

To validate laboratory methodologies that could be applied to the analysis of post-detonation nuclear debris, surrogate nuclear explosive debris (SNED) materials that enable benchmarking against other existing techniques are needed. However, realistic SNED is challenging to produce as these materials must simulate the diverse and complex properties of nuclear fallout, including physical (e.g., size, shape, density, color, etc.), chemical (e.g., stable elemental composition), and radiometric characteristics (e.g., short-lived fission products and other radionuclides).[6-8] Furthermore, for SNED to be useful as reference materials it must have well characterized and reproducible properties, especially with regards to incorporated radionuclide content. Surrogate debris materials must also be sufficiently homogenous within a batch to enable subsampling for intercomparisons and method validation across multiple laboratories.

Many techniques have been explored to create SNED including CO_2 laser irradiation[9], electrical discharge[10], and high temperature glass sintering[11, 12] While effective in producing materials that simulate many of the elemental and morphological characteristics of historic nuclear debris, these methods are high temperature approaches that can increase radionuclide fractionation during sample production. Sol-gel synthesis techniques have been explored as a method for SNED production as they provide tunability of many of the afore mentioned parameters.[12-14] and avoid high temperature thermal treatment. Recently, Lusk et al. demonstrated the ability to encapsulate and retain major fission products, with the exception of iodine and noble gases, within sol-gels.[14] Cooper et al. expanded upon that work by incorporating stable elements into

matrix glasses and reproducing the elemental and fresh fission product composition of historic NNSS debris.[15] Characterizing the retention of secondary constituents of sol-gels has been explored previously for various applications such photoluminescent[16, 17], photocatalytic[18, 19], and bioactive materials.[20-22] These studies all note the homogenous distribution of secondary chemical constituents into the sol-gel matrix. Despite these results, a rigorous characterization of the retention of fission products, present at much lower atom concentrations than stable elements previous reported, has not yet been studied and the homogeneity of these materials with respect to sample subdivision and across various production methods has not been assessed.

This work reports the characterization of fission product incorporation within sol-gel SNED materials. Specifically, the efficiency of doping a standardized radionuclide solution into a solid sol-gel matrix is quantified. Furthermore, the distribution of fission products within smaller and smaller subdivisions of a larger batch of material was characterized using gamma spectrometry. Finally, the effect of the sol deposition method on the homogeneity of fission products with respect to subdivision was measured.

Experimental

Fission Product Source Term

Fission products for these experiments were obtained via uranium photofission of a depleted uranium (DU) target and neutron irradiation of a highly enriched uranium (HEU) target. Briefly, fission products were produced via photofission were generated via the bremsstrahlung photon irradiation of approximately 1 g of DU at the Idaho State University's high-power S-band electron linear accelerator, as described previously.[23] Following irradiation and cooling, targets were shipped to Idaho National Laboratory (INL) where they were dissolved in 9 mL of concentrated nitric acid and the uranium was removed using a UTEVA column separation procedure described previously.[14, 23]

Fission products from neutron irradiation were produced at the Washington State University TRIGA research reactor. Following irradiation, the HEU target was processed at Pacific Northwest National Laboratory (PNNL) to isolate the fission products and subsequently sent to INL as a 5 mL 8 M nitrate solution. Aliquots of each fission product

solution were collected and characterized via gamma spectrometry for "total fissions", which describes the number of U atoms that fissioned in the sample by quantifying the molybdenum-99 (^{99}Mo) content and assuming a ^{99}Mo fission yield of 6.1%. The INL photofission and PNNL neutron fission samples were found to contain approximately $1x10^{15}$ and $4x10^{12}$ total fission, respectively. This metric is used to quickly describe approximate fission content in subsequent samples produced.

Sol-gel SNED Particle Production Method

Fission product baring silica sol-gel SNED particles were produced by combining tetraethyl orthosilicate (TEOS, 98% ACROS Organics), ethyl alcohol (200 proof HPLC grade, Sigma Aldrich) and nitric acid (HNO_3) containing the radionuclides to be incorporated, in a 3.2:3:20 ratio of TEOS:EtOH:HNO_3, respectively. This specific ratio was arrived at empirically to provide a rapid ambient gelation and drying time of 4-10 hours and is consistent with previously documented sol-gel behavior.[24] To this solution, an aliquot of the fission product solution containing $1x10^{12}$ – $1x10^{13}$ total fissions was added. The combined fission product and sol-gel precursor solution was then homogenized by agitation for 2 min using a blood vial rocker(LW Scientific), then deposited onto a hydrophobic FEP laminate surface (Cole-Parmer) in specific volume droplets from 1-10 μL depending on desired particle size and allowed to dry for 12 hr. Particles were then removed from the surface and thermally treated in a porcelain crucible in a muffle furnace at 400℃ for 30 minutes in air. Particles were then removed and allowed to cool prior to further analysis.

Evaluation of Quantitative Fission Product Encapsulation

Approximately 5 g of nominally 1.2 mm diameter sol-gel SNED particles containing approximately $1x10^{13}$ fissions were produced and used to evaluate the relative fission product encapsulation across the SNED production process. Relative fission product incorporation was characterized by measuring fission product quantities in the

initial precursor solution and comparing them with those measured following the production of the SNED, using gamma spectrometry.

Samples were quantified using an Ortec IDM-200-V High Purity Germanium gamma spectrometer (HPGe). Detector efficiency curves were constructed using calibration sources (^{137}Cs, ^{60}Co, and ^{152}Eu) at 10, 20, and 50 cm. Monte Carlo N Particle (MCNP) simulations were performed to match the calibration source measurements for the HPGe detector used. Once agreement between simulations and measurements was satisfactory, additional simulations were then used to extrapolate the detector efficiency curves to the specific source geometry and distance utilized during SNED sample measurements. Quantification of uncertainty for the SNED measurements involved 1) calibration source uncertainty, 2) interpolating efficiency between calibration source gamma-ray energies, and 3) sensitivity analyses for simulations based on slight changes in measurement position or attenuation through SNED sample materials. The uncertainty for each calibration source was 1% (1σ), and the total uncertainty for SNED measurements was approximately 3-5% (1σ) depending on the gamma-ray photopeak. Samples were placed at 200 cm from the face of the detector and measured for 14 h.

Evaluation of Fission Product Distribution Homogeneity with Sub-sampling

A 2 g aliquot of the previously mentioned 5 g sol-gel SNED sample was subdivided into 20 subsamples with masses between 0.10 and 0.77 g. The mass normalized fission product content of each fraction was then characterized by gamma spectrometry as described above and compared.

Evaluation of Particle Size and Sample Mass on Sub-sample Fission Product Homogeneity

Three SNED sol-gel samples were produced targeting 3 different particle diameters of approximately 500, 650 and 1200 μm. Actual particle size distributions for each of the 3 samples were characterized by optical microscopy. SNED samples were sent to be rigorously analyzed and counted at the Lawrence Livermore National

Laboratory (LLNL) Nuclear Counting Facility. At LLNL, from each of the three particle size batches, three mass aliquots of each 1-2 mg 15-20 mg, and 70-300 mg were weighed into polypropylene vials, yielding 18 total samples. Samples were dissolved prior to counting in order to ensure consistent counting geometry across sample sets. To each sample, a 3:1 (v/v) mixture of concentrated HNO_3: concentrated HF was added. The vials were capped and heated gently at about 60 C. Following full dissolution, which depending on particle size took anywhere from 1 to 16 h, the samples were diluted to 10 mL and transferred to a well-calibrated container for gamma spectrometry. Samples were counted at 8-12 cm from standard p-type high purity germanium detectors and analyzed using the GAMANAL software.[25] Fission products were normalized by mass of sol-gel particles or to the atoms of ^{99}Mo, which is a peak yield fission product. The internal and external uncertainties were compared across each triplicate size aliquot, considering nuclear counting and mass uncertainties.

Evaluation of Casting Method For SNED

The neutron activated fission product solution (5 mL solution containing $4x10^{12}$ fissions of fission product content in 8 M HNO_3) was used directly as the aqueous fraction of a sol-gel precursor solution, produced as described previously. The precursor solution was split into 2 aliquots and particles were cast as 10 µL droplets via two methods: 1. manual pipetting and 2. extrusion casting driven via peristaltic pump, both onto an FEP laminate hydrophobic surface. Particles cast via manual pipetting were cast over approximately 2 min using polypropylene pipettes tips, while casting via the extruder took approximately ten times longer at 20 min using Tygon and PTFE tubing extruded through polypropylene pipette tips. Particles were then removed from the surface and thermally treated in a muffle furnace at 400℃ for 30 minutes. Fission product content of each sample was characterized by gamma spectrometry, as previously described, and compared.

Results and discussion

The spherical shape and particle size was targeted during synthesis to simulate mid to near field aerodynamic nuclear fallout.[26, 27] A representative image of a sol-gel particle SNED sample is shown in Fig. 1. The particles produced here were hemi-spherical, due to casting on a surface, with diameters ranging between approximately 0.5 and 1.2 mm. Furthermore, the SNED densities were estimated based on a measured average particle hemi-spherical volume and particle masses at approximately 1.72 g/cm^3, which is consistent with densities of real nuclear fallout previously reported.[28]

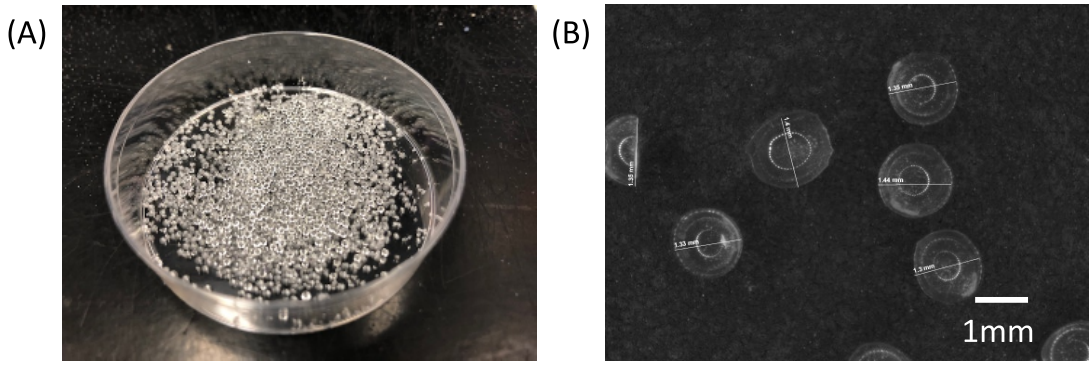

Fig. 1. (A) Approximately 500 mg of 1.2 mm sol-gel SNED particles. (B) Zoomed optical microscope image of 1.2 mm sol-gel SNED particles.

Relative Encapsulation of Radionuclide Content

The capacity to transfer and encapsulate the radionuclide content from a well characterized solution quantitatively into the sol-gel particles through the gelation and thermal treatment was assessed. This is an important metric in characterizing the viability of these simulants for their potential utility as reference standards.

To characterize the relative encapsulation, the radionuclide content of the SNED precursor fission product solution was characterized via gamma-ray spectroscopy prior to casting the particulate SNED. This measurement was then compared to a gamma measurement of the bulk final sol-gel simulant particles following casting and vitrification. A portion of the gamma spectra comparison between the original fission product solution and the final sol-gel simulant sample produced is shown in Fig**.** 2(see also Table S-1 in , Supporting Information, for complete fission product comparisons).

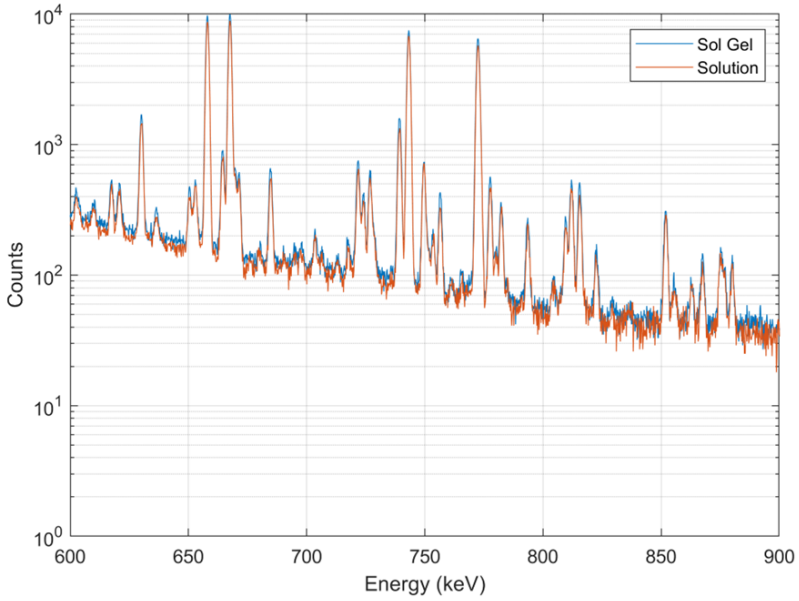

Fig. 2 Gamma Spectrum of original fission product solution and final sol-gel simulant particles plotted on the same axis between 600 and 900 keV.

The comparison of gamma spectra shows near perfect overlap between the fission product solution and the final sol-gel product indicating the radionuclide content was fully transferred to the sol-gel. A cosine similarity analysis was performed as a quantitative measure of the spectral similarity, where each spectrum is treated as a multi-dimensional vector and the cosine of the angle between them is calculated. Comparisons include the full structure of the spectra and thus account for peak locations, intensities, and background levels. Gamma spectra that are completely orthogonal will have a cos(θ) of 0 while perfectly overlapping spectra will have a cos(θ) of 1. The cosine similarity between the solution spectrum and a background spectrum yielded only a value of

0.5695. By contrast, the comparison between the sol-gel and the solution gamma spectra yielded a cosine value of 0.9995, confirming the agreement between the two spectra.

The activities of 11 specific fission products were compared between the fission product solution and sol-gel simulant particles. The ratio of the measured activity of each fission product in the solution and the simulant particles was used as a measure of encapsulation efficiency, with a value of 1 indicating quantitative encapsulation. These ratios are plotted relative to the mass number of the fission product in Fig. 3 and detailed table of the measured activities can be found in Table. S-1 in supporting information.

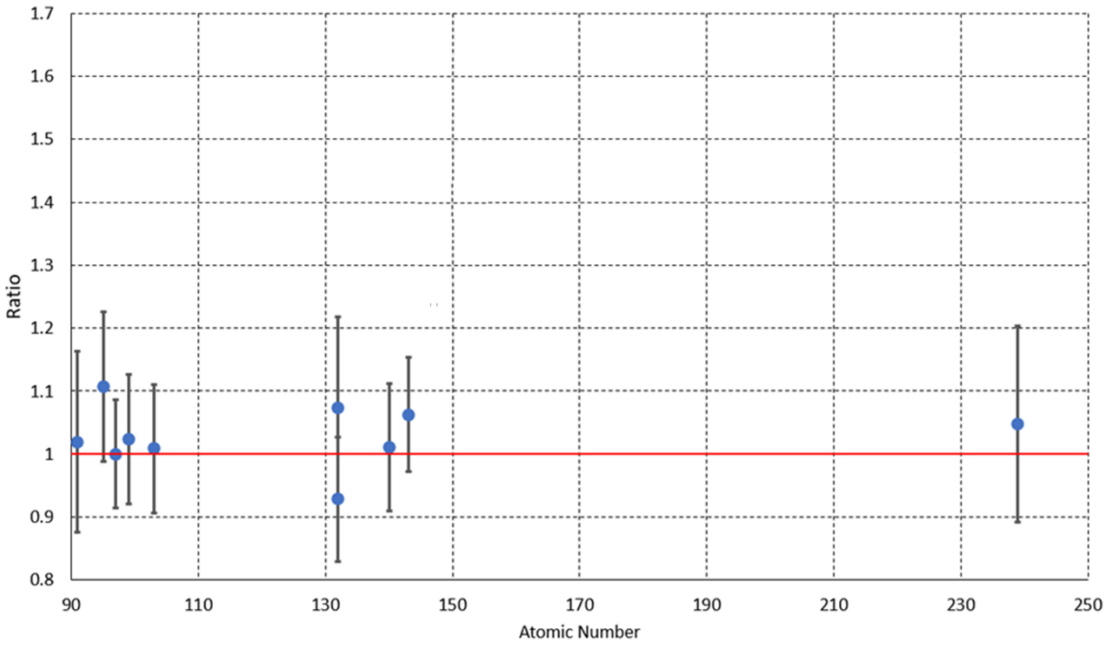

Fig. 3 Solution/sol-gel Ratio vs. atomic number of the radionuclide. With exception of Nd-147 all ratios are within 1σ of unity indicating a quantitative encapsulation of material in the sol-gel.

For most fission products analyzed, solution versus sol-gel activity ratios fell within 1σ uncertainty of unity. These data indicate a near quantitative relative transfer and encapsulation of each fission product in the final sol-gel simulant particles, within the fitting uncertainty of the gamma spectrum quantitation.

These data are representative of multiple (>10) fission product encapsulation characterization experiments conducted since 2021 conducted at INL. The individual results of each trial are shown in Table S-2 in supporting information. The aggregate

result of these encapsulation experiments shows an average encapsulation ratio of 1.04 ± 0.05, clearly demonstrating the quantitative radionuclide encapsulation capability of sol-gel based SNED.

Homogeneity With Respect to Sample Subdivision

The homogeneity of the sol-gel based SNED with respect to sample subdivisions is another important parameter to characterize for its potential use as a reference material for validation and benchmarking of nuclear forensic analytical methods.

The mass normalized activities of 4 fission products (Te-132, Ba-140, Nd-147, and Zr-95) were compared with their average activity measured across the 20 subsamples and are plotted in Fig. 4.

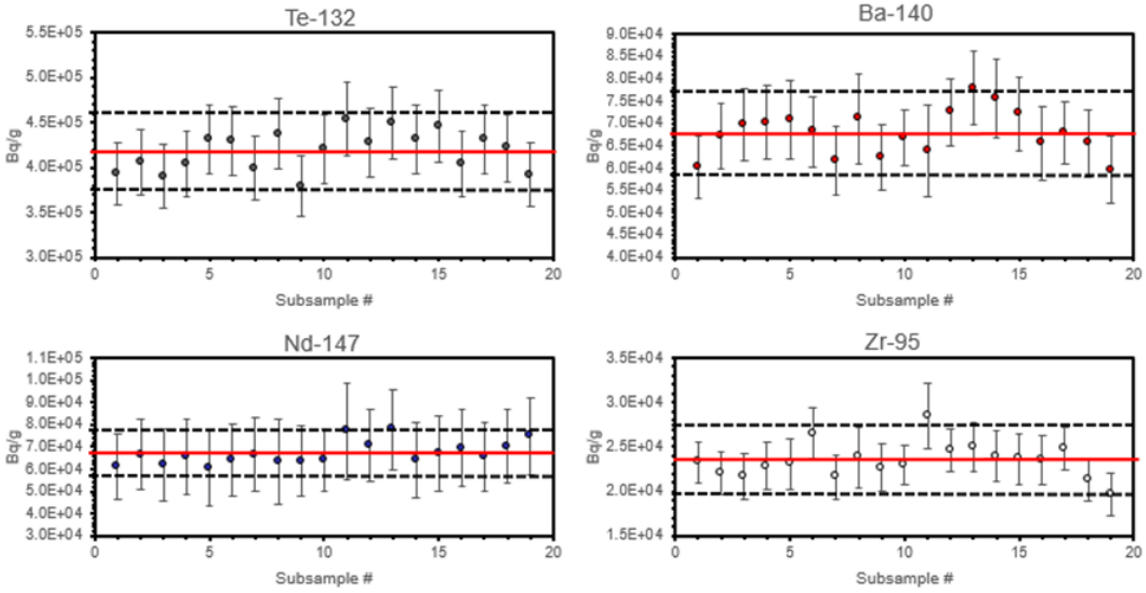

Fig. 4 Mass normalized fission product activity across 20 subsamples of a single sol-gel SNED sample. Red line represents the average activity and the dashed lines represent the 1σ bounds. Individual measurement uncertainties are also 1σ.

All mass normalized activities measured fell within measurement uncertainty of the calculated subsample weighted average. The relative standard deviation ranged from a low of 5.3% for Te-132 to a high of 7.6% for Ba-140. An analysis of the measurement uncertainty shows that the Ba-140 had a slightly higher measurement uncertainty by a factor of approximately 1.3x relative to the Te-132.

Effect of Sub-sample Mass on Homogeneity

The dependence of homogeneity on the sub-sample mass of the sol-gel SNED was explored. Samples were sub-divided into two mass ranges identified as a "mid-level" mass range with masses between 70-300 mg, and "low-level" mass range. The "low-level" mass range was sub-divided further into two ranges, 1-2 mg and 15-20 mg.

The relative standard deviation (RSD) and Birge ratios of fission product activities were used as a metric for judging the homogeneity of each sub-sample set. The homogeneity was tracked specifically for the fission products Ba-140, Mo-99, Ru-103, Te-132, and Zr-95. A representative table of the calculated RSDs are shown in Table 1 and the RSDs and Birge ratios for the "low-level" sub-sample set are shown in Table 2. The full data set can be found in Table S-3 and S-4 in supporting information.

Table 1. Fission product activity RSD across a representative triplicate sample set.

	Mid-Level Mass Range		Low-level Mass Range			
Mass	70-300 mg		1-2 mg		15-20 mg	
	N/^{99}Mo	A/g	N/^{99}Mo	A/g	N/^{99}Mo	A/g
^{140}Ba	3.06	5.01	0.01	5.14	0.57	0.69
^{99}Mo	N/A	3.77	N/A	5.14	N/A	0.37
^{103}Ru	2.45	4.95	2.04	4.7	6.21	5.88
^{132}Te	1.73	3.75	0.29	5.34	0.43	0.67
^{95}Zr	3.44	2.25	1.13	5.78	0.89	0.61

Table 2. Fission product activity Birge ratios across a representative triplicate sample set. Values that exceed unity indicate that the external variance across the triplicate set is greater than the internal measurement uncertainty.

Mass	1-2 mg		15-20 mg	
	N/^{99}Mo	A/g	N/^{99}Mo	A/g
^{140}Ba	0.01	1.18	0.77	0.9
^{99}Mo	N/A	1.17	N/A	0.43
^{103}Ru	1.08	0.99	4.6	4.32
^{132}Te	0.4	1.23	0.63	0.93
^{95}Zr	0.75	1.27	0.72	0.48

For most sets, the Birge ratios were close to unity, indicating a level of statistical consistency across each sample set, with no apparent correlation with the sample mass range. It is important to note that the Birge ratio is limited by the measurement uncertainty of the gamma spectrometry and mass measurements. Measurement uncertainties for the radionuclides analyzed here were generally less than 2%. A full breakdown of the internal measurement uncertainty for each sample is shown in Table S-5 of supporting information.

The RSDs ranged from 1% to 20%, however the majority of the variance came from 1-2 mg sample range, with the 15-20 mg sample range exhibiting much narrower RSDs on the order of 2-5%. For both metrics, the homogeneity of the sample is improved when normalized against Mo-99 versus a sample mass normalization. This is due to increased uncertainty associated with low-mass measurements of these particles. It is important to note that the measured RSDs for the 15-20 mg mass samples are approaching the internal measurement uncertainty which would represent the theoretical limit to the RSD. Relative standard deviations of radionuclide quantities the mid-level mass ranged from 2.25 to 5.01% for the mass normalized measurements. Again, the RSDs were generally lower and spanned a narrower range when quantities were normalized to ^{99}Mo with RSDs ranging from 1.73 to 3.44%.

Effect of Particle Size

Birge ratios and RSDs were also used to compare homogeneity as a function of particle size. SNED sample particle size distributions were characterized via optical microscopy and found to be 534 ± 11, 646 ± 11 and 1260 ± 24 μm, respectively.

At the 15-20 mg mass range, both the Birge ratio and the RSDs trended downward between the smallest and largest particle size which were 534 μm and 1250 μm respectively. This would be consistent with Poisson counting statistics given the larger solution volume sampling associated with increasing particle size. However, for most radionuclides, RSDs generally increased slightly at the intermediate particle size of 646 μm. This behavior may be anomalous, however, as only 3 particle sizes were interrogated, and the intermediate size is biased toward the smaller end of the size range examined. Thus, a test including more particle sizes and a wider size range would be

required to better elucidate the homogeneity versus particle size trend. These experiments will be the subject of a future study. The measured RSDs versus the particle size for each radionuclide is shown in Fig 5.

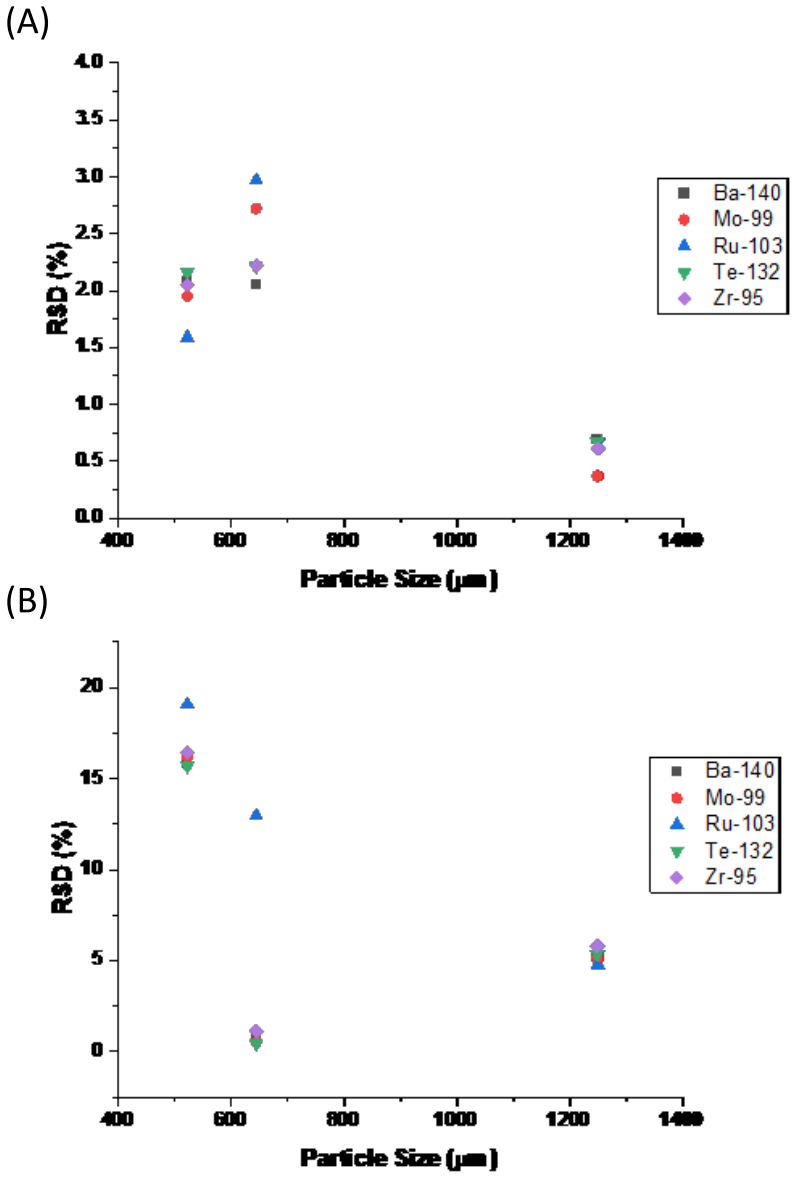

Fig. 5 (A) Measured RSDs versus 534, 646 and 1250 µm particles sizes for the 15-20 mg mass range. (B) Measured RSDs versus 534, 646 and 1250 µm particles sizes for the 1-2 mg mass range.

The homogeneity versus size trend is less apparent for the 1-2 mg mass range. However, the measured RSDs still trend toward decreased RSD at larger particle sizes.

Effect of Particle Casting Method

The effect of the particle casting time on the sample heterogeneity with respect to the radionuclide content was explored. Several factors relevant to the method could potentially contribute to heterogeneity. For example, the material in contact with solution (pipette tips, tubing, solution reservoir, etc.), may have varying affinities toward different fission products resulting in fission product fractionation and thus higher RSDs between sample replicates. The time dependence of the casting method may also play a role, with casting methods that require longer relative times potentially allowing for phase separation within the solution reservoir resulting in intra-sample heterogeneity. Manual pipetting and extrusion casting driven via peristaltic pump were used as comparative casting methods to study the effect of casting time on intra-sample heterogeneity, with casting times taking approximately 2 min and 20 min, respectively. Images of the manual pipettor and extruder are shown in Fig. 6.

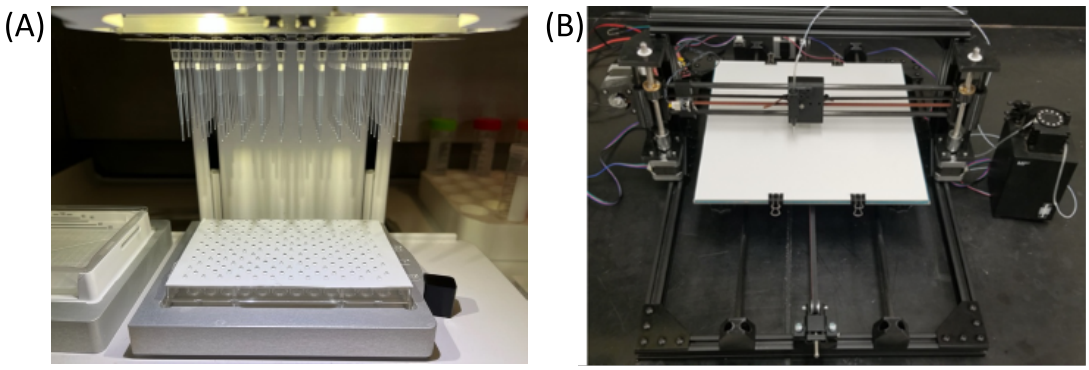

Fig. 6 (A) Manual pipette particle casting onto hydrophobic surface. (B) Peristaltic pump extrusion casting onto hydrophobic surface.

The RSDs of Ru-103 and Zr-95 activities were used as a measure of the intra-sample heterogeneity and compared between the two casting methods. Ruthenium and Zr were respectively chosen as representative volatile and refractory fissionogenic elements. Ruthenium, in particular, has been shown to be easily volatilized, when in nitrate solution form, during low temperature evaporation and annealing steps similar to those present during the sol-gel SNED production process.[29, 30]

The particle casting method did not seem to have an appreciable impact on the heterogeneity for Zr-95. The RSDs for Zr-95 were inversely correlated with sample mass. The manual pipette RSDs were measured at 18.5% for the 10 mg mass sample decreasing to approximately 1.7% for the 500 mg sample mass. A similar trend was seen in the extruded particles. For Ru-103 the relative standard deviation did not exhibit a correlation with sample mass, with an average deviation of 3% across all mass points for the extruded particles. However, the average RSD for Ru-103 was substantially larger for the manually pipetted particles, peaking at almost 100%. This may indicate a Ru-103 intra-sample heterogeneity that is dependent on particle casting time or solution contact surfaces. However, an important result is that despite the known volatility of Ru-103, potentially leading to the observed higher intra-sample heterogeneity, the extrusion-based casting method resulted in a much more homogenous sample with respected to Ru-103. The RSDs for all samples measured are presented in Table 3.

Table 3. Relative standard deviations for all particle samples measured for extruded and manually pipetted particles.

	Extruded Particles		Manually Pipetted Particles	
Nominal Subsample mass (mg)	^{95}Zr %RSD	^{103}Ru %RSD	^{95}Zr %RSD	^{103}Ru %RSD
10	14.7	1.7	18.51	86.5
50	6.5	4.9	6.0	99.9
100	2.6	2.5	1.8	30.0
500	3.52	3.5	1.7	34.0

These results show that the particle radionuclide heterogeneity is not appreciably increased by moving to the extrusion based casting method, allowing for future automation, which could substantially increase particle production throughput while decreasing potential radiation dosage to the chemist.

Conclusions

Results demonstrate both quantitative encapsulation of radionuclides into sol-gel based nuclear explosive debris simulants and homogeneity in the 2-5% range with respect to 15-20 mg sample subdivisions of the material. Simulant particle samples were shown to contain the entirety of their precursor radionuclide solution within the uncertainty of gamma spectrometry characterization. This demonstrates the ability to prepare simulant samples with targeted activity, radionuclide content and ratios. Furthermore, the samples can be prepared without appreciable loss of radioactive material. Sub-sample homogeneity was shown to be sample mass dependent with higher relative standard deviations being observed for sub-samples of lower mass. Despite this trend, relative standard deviations were still held to less than 7% for a 1-2 mg mass sub sample. Finally, the sub-sample homogeneity was not appreciably impacted by particle casting via peristaltic pump solution extrusion versus manual pipetting, which lays the foundation for a variety of automated SNED production methods for high-throughput production. The method presented here will allow for the production of targeted, homogenous sol-gel based SNED simulants to benchmark analytical techniques.

Acknowledgements

We would like to thank researchers at Pacific Northwest National Laboratory for providing a fission product sample produced at the Washington State University TRIGA reactor. We thank Brian Sammis from the LLNL Nuclear Counting Facility for counting support. We also thank Dr. Jon Stoner from the Idaho Accelerator Center for providing irradiation support for this work.

This work was funded by the Office of Defense Nuclear Nonproliferation Research and Development within the U.S. Department of Energy's National Nuclear Security Administration. This work was performed in part under the auspices of the U.S. Department of Energy by Lawrence Livermore National Laboratory under Contract DE-AC52-07NA27344. Neither the U.S. Government nor any agency thereof, nor any of their employees, makes any warranty, express or implied, or assumes any legal liability or responsibility for the accuracy, completeness, or usefulness of any information, apparatus, product, or process disclosed, or represents that its use would infringe on privately owned rights. References herein to any specific commercial product, process, or service by trade name, trademark, manufacturer, or otherwise, do not necessarily constitute or imply its endorsement, recommendation, or favoring by the U.S. Government or any agency thereof. Views and opinions of the authors expressed herein do not necessarily reflect those of the U.S. Government or any agency thereof.

Supporting Information

A document containing supporting information is included. This document contains the complete data of the 10 radionuclide fission products who's quantitative encapsulation was tracked via gamma spectrometry, a complete list of all surrogate debris production campaigns and the fission product encapsulation measured for each, the complete data set of the homogeneity statistical parameters measured for each particle subsample as a function of particle size and mass.

References

(1) Bellucci, J.; Simonetti, A. Nuclear forensics: searching for nuclear device debris in trinitite-hosted inclusions. *J. Radioanal. Nucl. Chem.* **2012**, *293* (1), 313–319. DOI: 10.1007/s10967-012-1654-9.

(2) Bellucci, J. J.; Simonetti, A.; Wallace, C.; Koeman, E. C.; Burns, P. C. Isotopic Fingerprinting of the World's First Nuclear Device Using Post-Detonation Materials. *Anal. Chem.* **2013**, *85* (8), 4195–4198. DOI: 10.1021/ac400577p.

(3) Davis, J. Post detonation nuclear forensics. *AIP Conference Proceedings* **2014**, *1596* (1), 206–209. DOI: 10.1063/1.4876471.

(4) Dunlop, W.; Smith, H. Post-Detonation Nuclear Forensics. *Arms Control Today* **2006**, *36* (8), 9.

(5) Stratz, S. A.; Gill, J. A.; Auxier II, J. D.; Hall, H. L. Modern Advancements in Post-Detonation Nuclear Forensic Analysis. *International Journal of Nuclear Security* **2016**, *2* (3), 6.

(6) Dardenne, Y. M.; Parker, W. E.; Knight, K. B. *Chemical Fractionation is not a Constant: Revisiting Bomb Vapor Chemistry*; Lawrence Livermore National Lab.(LLNL), Livermore, CA (United States), 2020, 3–20.

(7) Freiling, E. Radionuclide fractionation in bomb debris. *Science* **1961**, *133* (3469), 1991–1998.

(8) Izrael, Y. A. *Radioactive Fallout After Nuclear Explosions and Accidents*; Elsevier, 2002, 1-281.

(9) Liezers, M.; Fahey, A. J.; Carman, A. J.; Eiden, G. C. The formation of trinitite-like surrogate nuclear explosion debris (SNED) and extreme thermal fractionation of SRM-612 glass induced by high power CW CO2 laser irradiation. *J. Radioanal. Nucl. Chem.* **2015**, *304* (2), 705–715. DOI: 10.1007/s10967-014-3895-2.

(10) Dai, Z. R.; Crowhurst, J. C.; Grant, C. D.; Knight, K. B.; Tang, V.; Chernov, A. A.; Cook, E. G.; Lotscher, J. P.; Hutcheon, I. D. Exploring high temperature phenomena related to post-detonation using an electric arc. *J. Appl. Phys.* **2013**, *114* (20), 204901. DOI: 10.1063/1.4829660 (accessed 6/13/2024).

(11) Harvey, S. D.; Liezers, M.; Antolick, K. C.; Garcia, B. J.; Sweet, L. E.; Carman, A. J.; Eiden, G. C. Porous chromatographic materials as substrates for preparing synthetic nuclear explosion debris particles. *J. Radioanal. Nucl. Chem.* **2013**, *298* (3), 1885–1898. DOI: 10.1007/s10967-013-2563-2.

(12) Carney, K. P.; Finck, M. R.; McGrath, C. A.; Martin, L. R.; Lewis, R. R. The

development of radioactive glass surrogates for fallout debris. *Journal of Radioanalytical and Nuclear Chemistry* **2014**, *299* (1), 363–372. (accessed 2021/12/02/17:28:57). From Springer Link.
(13) Carney, K.; Finck, M.; McGrath, C.; Brush, B.; Jansen, D.; Dry, D.; Brooks, G.; Chamberlain, D. The development of radioactive sample surrogates for training and exercises. *J. Radioanal. Nucl. Chem.* **2013**, *296* (2), 769–773.
(14) Lusk, R.; Meiers, J.; Bucher, B.; Wall, N.; Forbush, S.; Carney, K.; Chichester, D. L.; Snow, M. Retention of radionuclides in sol–gel surrogate nuclear explosive debris. *J. Radioanal. Nucl. Chem.* **2023**, *332* (3), 683–689. DOI: 10.1007/s10967-022-08716-0.
(15) Diehl, G.; Cooper, J. T.; Mastren, T.; Holschuh, T. V.; Chichester, D. L.; Snow, M. Investigating sol–gel matrix loading capacity toward producing surrogate nuclear explosive debris with realistic composition. *J. Radioanal. Nucl. Chem.* **2024**, *333* (7), 3395–3405. DOI: 10.1007/s10967-023-09299-0.
(16) Mansuy, C.; Nedelec, J.-M.; Mahiou, R. Molecular design of inorganic scintillators: from alkoxides to scintillating materials. *J. Mater. Chem.* **2004**, *14* (21), 3274–3280, 10.1039/B405402D. DOI: 10.1039/B405402D.
(17) Mansuy, C.; Mahiou, R.; Nedelec, J. M. A New Sol−Gel Route to Lu2SiO5 (LSO) Scintillator: Powders and Thin Films. *Chem. Mater.* **2003**, *15* (17), 3242–3244. DOI: 10.1021/cm034412t.
(18) Akpan, U. G.; Hameed, B. H. The advancements in sol–gel method of doped-TiO2 photocatalysts. *Applied Catalysis A: General* **2010**, *375* (1), 1–11. DOI: https://doi.org/10.1016/j.apcata.2009.12.023.
(19) Navío, J. A.; Colón, G.; Macías, M.; Real, C.; Litter, M. I. Iron-doped titania semiconductor powders prepared by a sol–gel method. Part I: synthesis and characterization. *Applied Catalysis A: General* **1999**, *177* (1), 111–120. DOI: https://doi.org/10.1016/S0926-860X(98)00255-5.
(20) Baikousi, M.; Agathopoulos, S.; Panagiotopoulos, I.; Georgoulis, A. D.; Louloudi, M.; Karakassides, M. A. Synthesis and characterization of sol–gel derived bioactive CaO–SiO2–P2O5 glasses containing magnetic nanoparticles. *J. Sol-Gel Sci. Technol.* **2008**, *47* (1), 95–101. DOI: 10.1007/s10971-008-1720-5.
(21) Faure, J.; Drevet, R.; Lemelle, A.; Ben Jaber, N.; Tara, A.; El Btaouri, H.; Benhayoune, H. A new sol–gel synthesis of 45S5 bioactive glass using an organic acid as catalyst. *Materials Science and Engineering: C* **2015**, *47*, 407–412. DOI: https://doi.org/10.1016/j.msec.2014.11.045.
(22) Vafa, E.; Bazargan-Lari, R.; Bahrololoom, M. E. Synthesis of 45S5 bioactive glass-ceramic using the sol-gel method, catalyzed by low concentration acetic acid extracted from homemade vinegar. *Journal of Materials Research and Technology* **2021**, *10*, 1427–1436. DOI: https://doi.org/10.1016/j.jmrt.2020.12.093.
(23) Snow, M. S.; Ward, J.; Bucher, B.; Cooper, J. T.; Kinlaw, M.; Cárdenas, E.; Horkley, J.; Town, H.; Finck, M.; Carney, K. Rapid Separation of Photofissioned Uranium Products via a Single-Pass Multiplexed Chromatographic Fission Product Separation System. *Anal. Chem.* **2021**, *93* (8), 3770–3777. DOI: 10.1021/acs.analchem.0c04130.
(24) Brinker, C. J.; Scherer, G. W. CHAPTER 5 - Gelation. In *Sol-Gel Science*, Brinker, C. J., Scherer, G. W. Eds.; Academic Press, 1990; pp 302–355.
(25) Gunnink, R.; Niday, J. B. *COMPUTERIZED QUANTITATIVE ANALYSIS BY GAMMA-RAY SPECTROMETRY. VOLUME I. DESCRIPTION OF THE GAMANAL PROGRAM*; UCRL-51061(Vol.1); United States, 1972, 78 DOI: 10.2172/4696896.

(26) Adams, C. E.; Farlow, N. H.; Schell, W. R. The compositions, structures and origins of radioactive fall-out particles. *Geochim. Cosmochim. Acta* **1960**, *18* (1), 42–56. DOI: https://doi.org/10.1016/0016-7037(60)90016-8.
(27) Larson, K. H.; Neel, J. W.; Hawthrone, H. A.; Mork, H. M.; Rowland, R. H.; Baurmash, L.; Lindberg, R. G.; Olafson, J. H.; Kowalewsky, B. W. *DISTRIBUTION, CHARACTERISTICS, AND BIOTIC AVAILABILITY OF FALLOUT, OPERATION PLUMBBOB. Projects 37.1, 37.2, 37.2a, 37.3, and 37.6*; WT-1488; United States, 1966, 1–281 DOI: 10.2172/4472210.
(28) Lewis, L.; Knight, K.; Matzel, J.; Prussin, S.; Zimmer, M.; Kinman, W.; Ryerson, F.; Hutcheon, I. Spatially-resolved analyses of aerodynamic fallout from a uranium-fueled nuclear test. *Journal of environmental radioactivity* **2015**, *148*, 183–195.
(29) Hölgye, Z.; Křivánek, M. On the volatility of ruthenium. *J. Radioanal. Chem.* **1978**, *42* (1), 133–141. DOI: 10.1007/BF02520633.
(30) Rudisill, T. *Ruthenium Volatiliazation During Dissolution of Spent Nuclear Fuels in H-Canyon Dissolvers*; SRNL--TR-2018-00073; Savannah River Site (SRS), Aiken, SC (United States), United States, 2019, https://www.osti.gov/biblio/1504625DOI: 10.2172/1504625.